Evaluating safety at sea by comparing numerical accuracies of ship motions

Sasa, Kenji
Terada, Daisuke
Shiotani, Shigeaki
Wakabayashi, Nobukazu

(Citation)
Journal of maritime researches,3(1):61-82

(Issue Date)
2013-03

(Resource Type)
departmental bulletin paper

(Version)
Version of Record

(JaLCDOI)
https://doi.org/10.24546/81006887

(URL)
https://hdl.handle.net/20.500.14094/81006887

Journal of Maritime Researches Vol. 3, No. 1 March 2013: 61-82.

EVALUATING SAFETY AT SEA BY COMPARING NUMERICAL ACCURACIES OF SHIP MOTIONS

Kenji SASA[*]
Daisuke TERADA[**]
Shigeaki SHIOTANI[**]
Nobukazu WAKABAYASHI[***]

ABSTRACT

The safety of maritime transportation should be ensured. However, the methods currently used to determine whether or not to cancel ship services are insufficient. A numerical simulation of ship motions was constructed using the coastal network wave database, NOWPHAS (Nationwide Ocean Wave network for Ports and HArbourS). A domestic ferry service, which navigates in the Pacific Ocean, was set as the object of this study. Field observations of ship motions were implemented against a 5,000DWT class domestic ferry when typhoons approached Japan. The accuracy of ship motions obtained using two types of simulation methods were verified. Finally, this study reveals the factor that controls the accuracy of ship motions.

Keywords: ship motions, numerical simulation, coastal wave database, safety of transportation, evaluation of hydrodynamic forces, impulse response

[*] Associate Professor, Graduate School of Maritime Sciences, Kobe University. 5-1-1 Fukaeminamimachi, Higashinada ku, Kobe shi, Hyogo, 658-0022, Japan. Email : sasa@maritime.kobe-u.ac.jp
[**] Researcher, National Research Institute of Fishery Engineering, 7620-7, Hasaki, Kamisu-shi, Ibaraki, 314-0408, Japan. Email : dterada@affrc.go.jp
[***] Professor, Graduate School of Kobe University. 5-1-1 Fukaeminamimachi, Higashinada ku, Kobe shi, Hyogo, 658-0022, Japan. Email : shiotani@maritime.kobe-u.ac.jp
[****] Professor, Graduate School of Maritime Sciences, Kobe University, 5-1-1 Fukaeminamimachi, Higashinada ku, Kobe shi, Hyogo, 658-0022, Japan. Email : waka@cs.maritime.kobe-u.ac.jp

1. INTRODUCTION

More than ninety percent of global cargo is currently transported by sea. Safe maritime transportation is a high priority at all times. Many studies have focused on the motions of moored ships due to long period waves in harbours facing the open seas (Shiraishi et al., 1996 and 1999). Furthermore, other studies have focused on ship motions when ships are entering a harbour or anchoring offshore (Sasa et al., 2005 and 2006). While ships are underway, suitable navigation routes are selected as the weather routing (James, 1957). However, the influence of ship motions has not yet been considered in detail. Although there are many studies of ship motions in the ocean from the viewpoint of seaworthiness (Okusu, 1996), they mainly involve frequency domain analysis. Most domestic ferry lines do not have effective ways to determine whether to cancel service in stormy weather. The individual responsible for canceling such services depends on intuition and experience, and sometimes fails to predict oceanographic conditions or ship motions. Any error in judgment has the potential to result in damage to cargo or casualty of the vessel. Few studies have involved comparisons of observed ship motions in a time series while the ships are underway in irregular waves. In Japan, the Nationwide Ocean Wave information network for Ports and HArbourS (NOWPHAS) (Nagai et al., 1997) was established for the purpose of constructing safe harbours. This system is used to evaluate safety in port construction and operations from various aspects in the field of coastal engineering. It is also effective for the estimation of ship motions underway. First of all, observing ship motions of domestic ferries in the Pacific Ocean has been carried out for two years, when typhoons approach to Japan. Observational data clearly demonstrates the characteristics of ship motions. The modeling of numerical simulations is carried out to verify observed ship motions with the coastal wave database. The simulated results show that there are some parameters that influence the accuracy of reproduction. Finally, the cancellation of domestic ferry services is determined with the use of a network coastal wave database.

2. CURRENT STATUS OF FERRY OPERATIONS

For navigation purposes, ship operators are always cognizant of changing oceanographic conditions. In particular, car ferries or RO/RO(Roll on/Roll off) ships load passengers and vehicle cargos, which are not acceptable under conditions of large amplitude ship motions. These vessels must operate in open seas without causing large motions or impulse forces. A study of cargo management by domestic ferries (Kobayashi et al., 2004) revealed that impact damage or collapse against vehicle cargos sometimes occurs if pitch or roll motions are exceptionally large. The current procedures for cargo management are not sufficient under such conditions, even though vehicles are secured with more wire lashings than are used in usual navigation. Furthermore, ship operators rely on their experience and knowledge of the daily

forecasted wave height distribution. The present criteria for the operation of domestic ferry liners are shown in Table 1. As reported earlier, ferry operation is determined on the basis of significant wave height. The relationship between ship motions and waves is extremely complex, especially when a vessel is underway. The complexity results in the heavy reliance on the ship operator's experience and intuition. Fig. 1 shows the location of navigation route and wave observation points here.

Table 1 Present criterion of ship operations

Topic	Comment
Criterion of ferry service	Ferry service can generally be provided until the significant wave height exceeds 4m. However, the steps for cancellation must be very specific when typhoons are involved.
Situation of ship motions	Pitch motion becomes larger in head seas during navigation. As ferries enter a harbour, the roll and yaw motions increase in intensity near the breakwaters.
Damage of cargos	Cargo is sometimes damaged by the shock due to large ship motions.

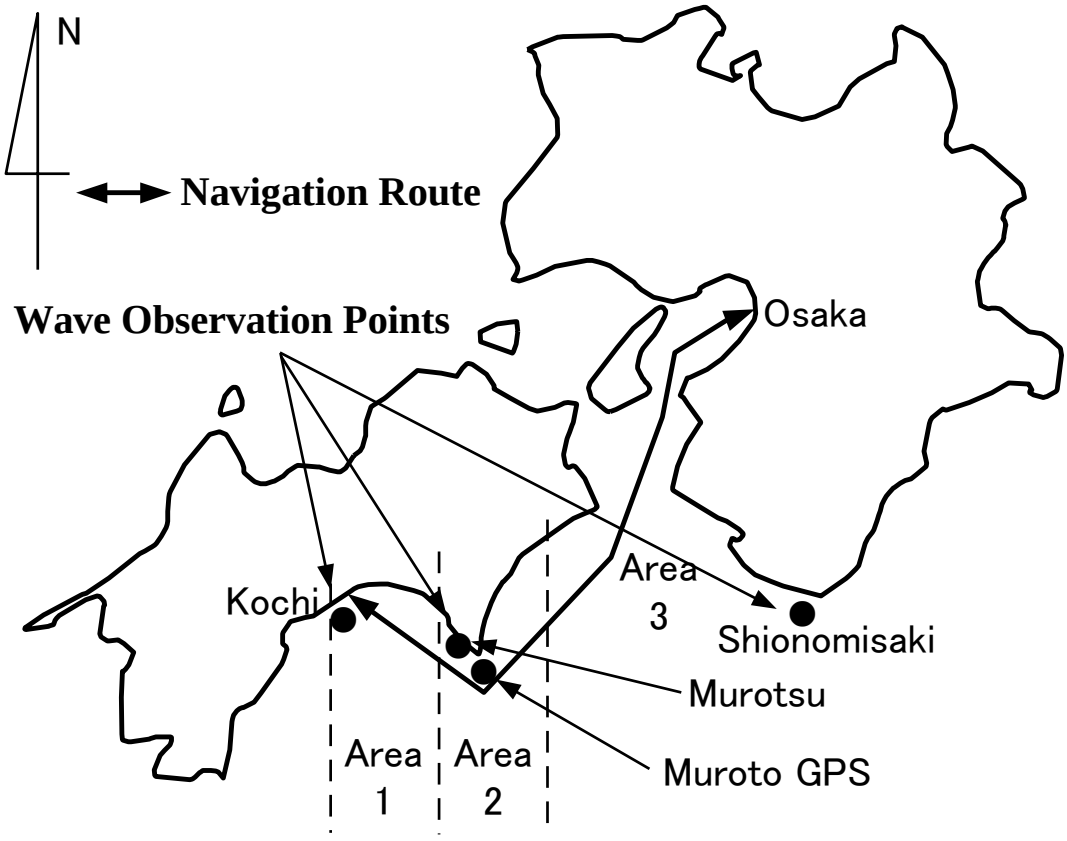

Fig. 1 General navigation route of a ferry with wave observation points

3. FIELD OBSERVATION OF SHIP MOTIONS UNDERWAY

3.1 Conditions of Field Observation

As reported earlier, presently there is no effective system or database for determining when to cancel shipping services. As a result, it is difficult to establish effective operational criteria. Ship motions while the ferry is underway are inevitable in heavy weather. For the purposes of this study, field observations of ship motions were undertaken for domestic ferries in the 5,000DWT class for 2003-2004. Fig. 1 shows the general navigation route of the ferry with the coastal wave observation points of NOWPHAS. The route is located between Osaka and Kochi in Western Japan facing the Pacific Ocean. Swells sometimes propagate into the navigation route as a result of typhoons. As shown in the figure, it is characteristic that the ferry course is altered with large angles off Murotsu point. This means that encounter frequency varies greatly because of the large variation of relative wave directions. The main dimensions of the ferry are 109m length between perpendiculars, 21m breadth, 4.5m draft, 6,032t displacement, and 1.4m metacenter height. Ship motions are observed by the measurement system, which consists of a GPS, an optical fiber gyro, and a gyro compass (Sasa, et al., 2003).

3.2 Characteristics of Observed Ship Motions

The main output parameters of the measurement system are the ship's position, course, motions, and velocities in 6 modes. These data are recorded every 0.2s during navigation. The average navigation time is approximately 9 hours between Osaka and Kochi. The size of obtained data is too large to directly analyze them at once. The observed data is divided into three regions, as shown in Fig. 1. According to a ferry captain, ship motions tend to grow around Murotsu and Kochi. Wave heights, especially, tend to amplify offshore of Cape Muroto (Kobayashi, et al., 2005). Here, the discussion of ship motions is primarily limited to those in area 2. The relative wave direction is defined as shown in Fig. 2. Observed data of ship motions include the ship's heading in each instance. The wave database, NOWPHAS, offers main wave directions every 20 minutes or 2 hours. This makes it possible to estimate the relative wave direction. Figs. 3-4 show the observed pitch motion, ship's velocity, and relative wave direction around Cape Muroto. A pitch of 4-5 degrees is appeared in both cases. The ship's velocity is smaller in Fig. 3 than that in Fig. 4. The speed shown in Fig. 3 is obviously slower than that of typical navigation. These results indicate that high waves and strong winds make it difficult to maintain a normal velocity of approximately 15-20 knots. The speed is one of the most important factors determining encounter frequency.

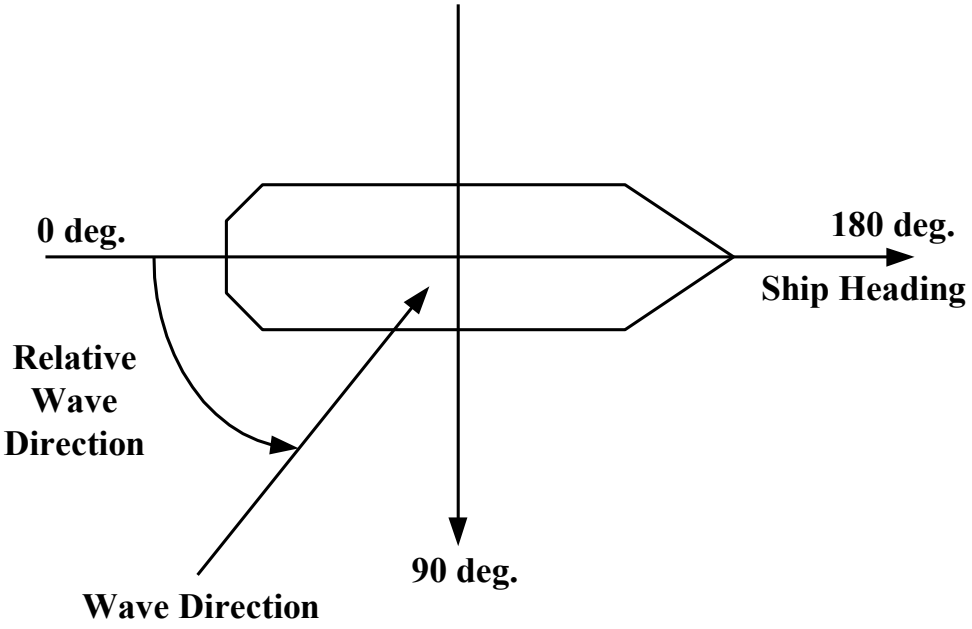

Fig. 2 Definition of relative wave direction

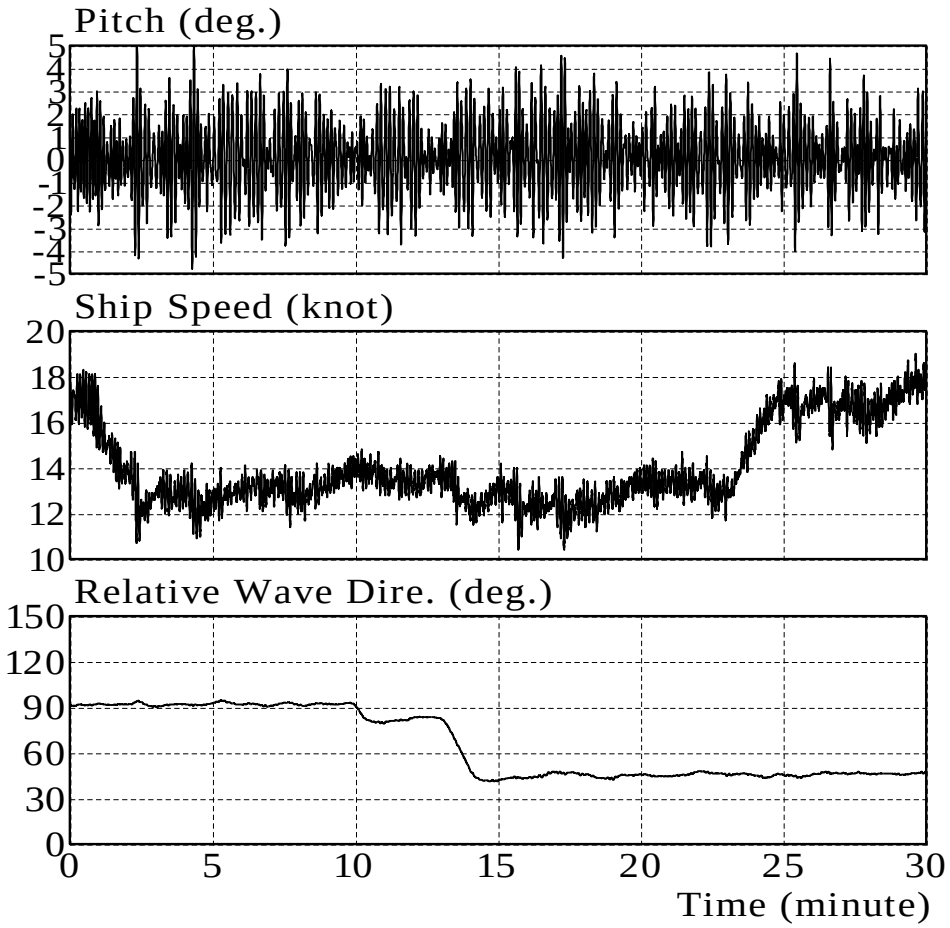

Fig. 3 Observed pitch motion, ship speed, and relative wave direction near Cape Muroto (September 21-22, 2002)

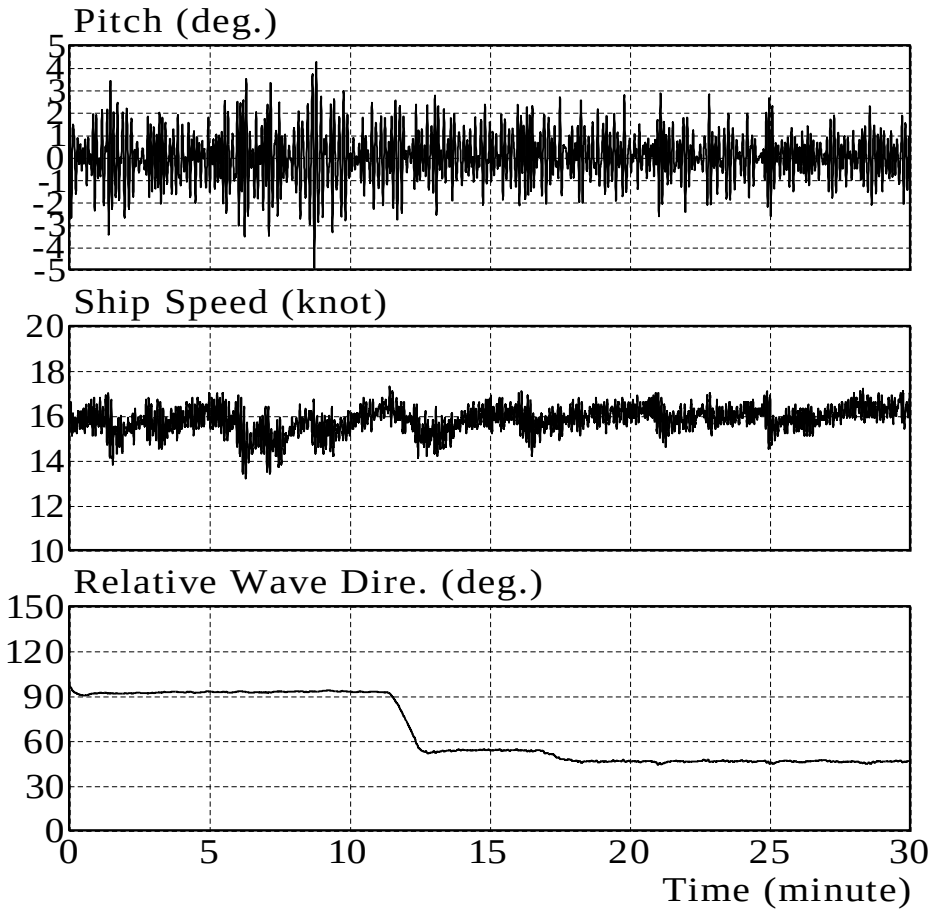

Fig. 4 Observed pitch motion, ship speed, and relative wave direction near Cape Muroto (July 30, 2004)

3.3 Relation between Coastal Waves and Ship Motions

It is imperative that the relationship between ship motions and waves be understood. It is not easy to observe waves surrounding a ship that is underway while using the currently available methods; furthermore, doing so incurs very high costs. NOWPHAS has been operational throughout Japan in recent decades. It includes 54 observation points. Many of them are located in coastal zones of the Pacific Ocean and the Sea of Japan. These points allow NOWPHAS to effectively analyze the relationship of motions of domestic ferries that are underway in coastal areas. The application of the NOWPHAS seems to be effective for estimating ship motions in this study. As shown in Fig. 1, there are three observation points (Murotsu, Muroto GPS, and Kochi) near the navigation route. Fig. 5 shows an observed time series of surface elevation at the Murotsu and the Muroto GPS. Frequency spectra of waves are compared with those of pitch motions shown in Figs. 3-4. The analyzed spectra are shown in Fig. 6.

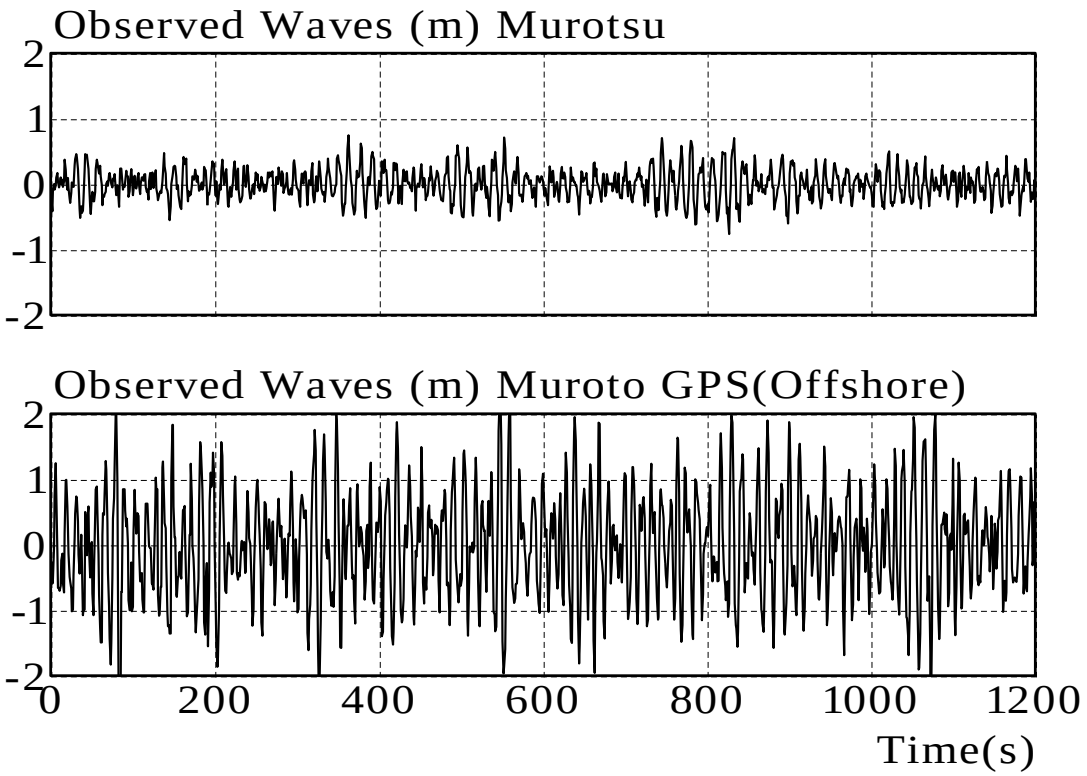

Fig. 5 Observed time series of surface elevation at Murotsu and Muroto GPS (0:00 July 30, 2004)

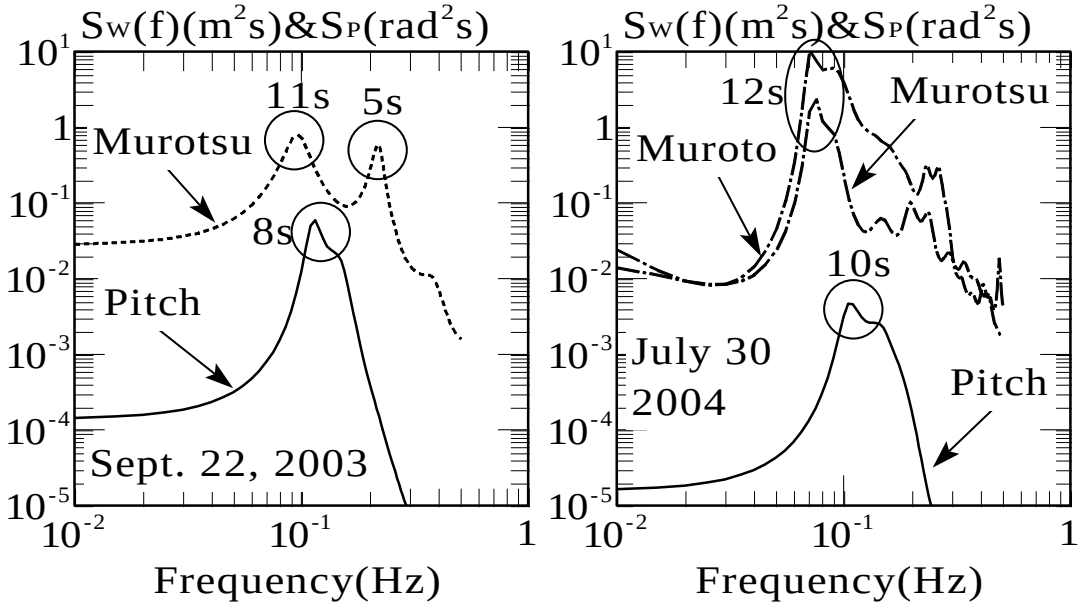

Fig. 6 Comparison of spectra of waves and pitch motions

In Fig. 5, wave amplitudes are quite different between Murotsu and Muroto GPS. The topography may affect the difference of wave height near the two points. In the left-hand section of Fig. 6, the wave spectrum has twin peaks around 11s and 5s, while

the pitch motion is around 8s. Swell and wind wave components coexist in this case. On the other hand, there is a spectrum peak at around 12s in the wave and 10s in the pitch motion in the right-hand section. The peak frequencies of waves are quite different from each other, although the ship motions are almost identical. Peak frequencies or ship speeds are known to vary from case to case, even though the ferry navigates in the same area of the sea. When ship motions underway are considered, the properties of motions are decided by the encounter frequency, which is expressed as follows:

$$\sigma_E = \sigma_W - kV\cos\alpha \quad , \tag{1}$$

where σ_E is the encounter frequency, σ_W is the angular frequency of waves, k is the wave number, V is the ship speed, and α is the relative wave direction. From the observation database, the relative wave direction or the ship speed is not constant, and neither is the wave frequency. This means that the encounter frequency is complex, and thus an accurate prediction of ship motions is nearly impossible on the basis of the forecasted wave height distribution alone. An accurate method for estimating ship motions as a result of coastal waves is required before making a decision to cancel ferry services.

4. NUMERICAL ESTIMATION OF LONGITUDINAL SHIP MOTIONS UNDERWAY USING COASTAL WAVES

Numerical simulations are necessary to estimate ship motions using coastal waves. There are few studies on the verification of accuracy of observed ship motions under severe seas in a time domain, although there are many studies on the numerical analysis of ship motions (Kashiwagi, 1997 and 2000) in the field of naval architecture. Here, ship motions are reproduced for a comparison of observed cases in a time domain after two types of equations of motions were constructed.

4.1 Coordinate System and Numerical Models

The coordinate system is defined in Fig. 7. Longitudinal motions are analyzed here because they can be separated from lateral motions on the assumption of the linear theory. Heave motion, X_1, and pitch motion, X_2, occur around the gravity point when the ship is underway with forward velocity, V. Wave forces and moments are calculated on the assumption of the small amplitude wave theory. A New Strip Method (NSM) was used as a practical method for calculating hydrodynamic coefficients and wave-exciting forces. When ship motions during long navigation are studied, they are usually analyzed in the frequency domain. In other words, simulated motions of ships that are underway are not compared with those observed in detail in a time domain.

Here, the accuracy of numerical simulations is discussed as the reproduction of a time series.

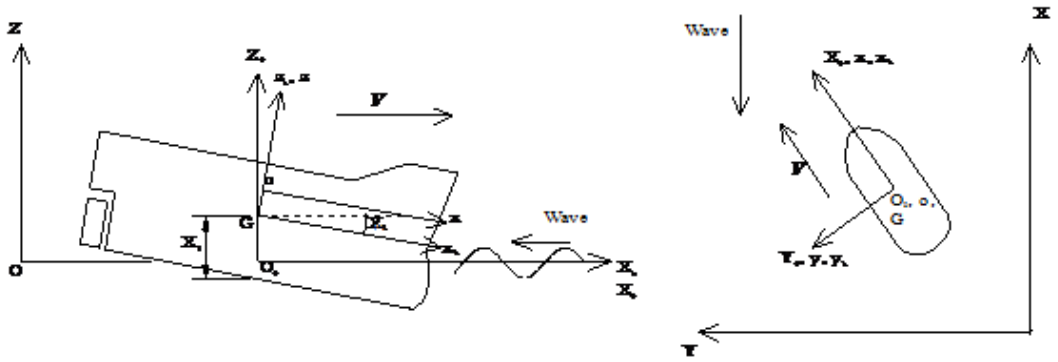

Fig. 7 Coordinate system of ship motion analysis

4.2 Equations for Motions of Ships that are in Underway

There are various methods of numerical simulations of ship motions (Okusu, 1996). Two time-domain analysis methods, the Constant Coefficient (CC) and the Convolution Integral (CI), are used here to verify the accuracy of the time series.

(1) Constant Coefficient (CC) Method

This is the equation of motions in which the inertia force and wave damping force are expressed as constant values in the mean wave period, T_{mean} (Ueda, 1984):

$$\sum_{i=1}^{2}\left(M_{ii}+A_{ij}\left(\sigma_{Emean}\right)\right)\ddot{X}_j(t)+\sum_{i=1}^{2}B_{ij}\left(\sigma_{Emean}\right)\dot{X}_j(t)+\sum_{i=1}^{2}C_{ij}X_j(t)=F_{WVj}(t)$$

$$(i, j=1, 2), \quad (2)$$

where M is the ship's mass, $A(\sigma_{Emean})$ and $B(\sigma_{Emean})$ are the added mass and wave damping coefficient, respectively, C is the restoring force coefficient, $F_{WV}(t)$ is the wave-exciting force, $X(t)$ is the displacement of ship motion, and t is the time. σ_{Emean} is the encounter frequency for the mean wave period, which can be obtained by Eq. 1. Hydrodynamic coefficients $A(\sigma_{Emean})$ and $B(\sigma_{Emean})$ are obtained as follows:

$$\begin{aligned}
&A_{11}(\sigma)=\int_L M_H(\sigma)dx \quad , \quad A_{12}(\sigma)=A_{21}(\sigma)=-\int_L xM_H(\sigma)dx \\
&A_{22}(\sigma)=\int_L x^2 M_H(\sigma)dx \quad , \\
&B_{11}(\sigma)=\int_L N_H(\sigma)dx \quad , \quad B_{12}(\sigma)=B_{21}(\sigma)=-\int_L xN_H(\sigma)dx
\end{aligned} \quad (3)$$

$$B_{22}(\sigma) = \int_L x^2 N_H(\sigma) dx \quad , \tag{4}$$

where $M_H(\sigma)$ and $N_H(\sigma)$ are two-dimensional added mass and wave damping coefficient at angular frequency, σ, respectively.

(2) Convolution Integral (CI) Method

Some studies (Shiraishi et al., 1999) have revealed that an impulse response should be considered to reproduce moored ship motions. That is the reason that some kinds of forces act on ships with various time periods. If Eq. 2 is used, radiation forces are represented as those at a particular frequency, such as the significant wave period. Numerical modeling of longitudinal motions has already been derived (Saito et al., 1992). However, it does not consider the shape of the ship's fore and aft. It also focuses on ship motions only in the longitudinal wave direction. The velocity potential, ϕ_{rz}, is obtained as the convolution integral between ship velocities and impulse response, if any ship section has motions.

$$\phi_{rz} = \varphi_z(y,z;x)U(t) + \int_0^t \chi_z(y,z;x,t-\tau)U(\tau)d\tau \quad , \tag{5}$$

where $\varphi_z(y,z;x)$ corresponds with the flow area while the ship is in impulse motions, $\chi_z(y,z;x,t-\tau)$ corresponds with the flow area in which the disturbance propagates in space and time after the impulse finishes. $\delta(t)$ is the delta function. If these are integrated along the ship's section, the two-dimensional constant added mass, $M_H(\infty)$, and the retardation function, $K_H(t)$, are derived as follows:

$$M_H(\infty) = -\rho \int_{-b}^{b} \varphi(y,z;x) dy \quad , \tag{6}$$

$$K_H(t) = -\rho \int_{-b}^{b} \frac{\partial \chi_z(y,z;x,t)}{\partial t} dy \quad , \tag{7}$$

where ρ is the density of sea water. The two-dimensional retardation function, $K_H(t)$, is expressed as follows:

$$K_H(t) = \frac{2}{\pi} \int_0^{\infty} N_H(\sigma) \cos \sigma t d\sigma \tag{8}$$

The fluctuating pressure against the ship hull is derived by Bernoulli's linear equation as follows:

$$p_{rz} = -\rho\left[\frac{\partial}{\partial t} - V\frac{\partial}{\partial x}\right]\phi_{rz} \tag{9}$$

The entire radiation force, $F_R(t)$, and moment, $M_R(t)$, can be shown as follows. Here, the force and moment are derived by considering the shape of the ship's fore and aft.

$$\begin{aligned}
F_R(t) &= \int_L \int_{-b}^{b} p_{rz}\, d\, y\, d \\
&= -\int_L M_H(\infty) dx \ddot{X}_1(t) - \int_L \int_0^t K_H(t-\tau)\dot{X}_1(\tau) d\tau dx \\
&+ V\int_L \frac{\partial M_H(\infty)}{\partial x} dx \dot{X}_1(t) \\
&+ V\int_L \int_0^t \frac{\partial K_H(t-\tau)}{\partial x} X_1(\tau) d\tau dx \\
&+ \int_L \{xM_H(\infty)\} dx \ddot{X}_2(t) + V\int_L \int_0^t \{xK_H(t-\tau)\}\dot{X}_2(\tau) d\tau dx \\
&- V\int_L \int_0^t \frac{\partial\{xK_H(t-\tau)\}}{\partial x} X_2(\tau) d\tau dx \\
&- 2V\int_L \int_0^t K_H(t-\tau) X_2(\tau) d\tau dx \\
&+ V^2 \int_L \int_0^t \frac{\partial K_H(t-\tau)}{\partial x} \cdot \left[\int_0^\tau X_2(s) ds\right] d\tau dx \qquad ,
\end{aligned} \tag{10}$$

$$\begin{aligned}
M_R(t) &= \int_L \{xM_H(\infty)\} dx \ddot{X}_1(t) \\
&+ \int_L \int_0^t \{xK_H(t-\tau)\}\dot{X}_1(\tau) d\tau \\
&- V\int_L \left[x\frac{\partial M_H(\infty)}{\partial x}\right] dx \dot{X}_1(t)
\end{aligned}$$

$$
\begin{aligned}
&-V\int_L\int_0^t\left[x\frac{\partial\{K_H(t-\tau)\}}{\partial x}\right]X_1(\tau)d\tau dx\\
&-\int_L\left\{x^2M_H(\infty)\right\}dx\ddot{X}_2(t)\\
&-V\int_L\int_0^t\left\{x^2K_H(t-\tau)\right\}\dot{X}_2(t)d\tau\\
&+V\int_L\int_0^t\left[x\frac{\partial\{xK_H(t-\tau)\}}{\partial x}\right]X_2(\tau)d\tau dx\\
&+2V\int_L\int_0^t\{xK_H(t-\tau)\}X_2(\tau)d\tau dx\\
&-V^2\int_L\int_0^t\left[x\frac{\partial K_H(t-\tau)}{\partial x}\right]\cdot\left[\int_0^\tau X_2(s)ds\right]d\tau dx
\end{aligned}
\tag{11}
$$

It has already been shown that retardation functions in the diffraction problem do not satisfy the law of causality because of the dispersibility of waves. Here, the impulse response is not considered in diffraction forces. Equations of motions are expressed as follows:

$$
\begin{aligned}
&\sum_{i=1}^{2}\left(M_{ii}+m_{ij}(\infty)\right)\ddot{X}_j(t)+\sum_{i=1}^{2}\int_{-\infty}^{t}K_{ij}(t-\tau)\dot{X}_j(\tau)d\tau\\
&+\sum_{i=1}^{2}C_{ij}X_j(t)+\sum_{i=1}^{2}D_{ij}+\sum_{i=1}^{2}E_{ij}=F_{WVj}(t)
\end{aligned}
\qquad (i,\ j=1,2) \tag{12}
$$

where $m(\infty)$ is the constant added mass, $K(t)$ is the retardation function, and D and E are added terms due to fore and aft shape of the ship. These variables can be expressed as follows:

$$K_{ij}(t)=\frac{2}{\pi}\int_0^\infty B_{ij}(\sigma)\cos\sigma t d\sigma \quad , \tag{13}$$

$$m_{ij}(\infty)=A_{ij}(\sigma)+\frac{1}{\sigma}\int_0^\infty K_{ij}(t)\sin\sigma t dt \quad , \tag{14}$$

$$
\begin{aligned}
D_{1j}&=-V\int_L\frac{\partial M_H}{\partial x}dx\dot{X}_1(t)\\
&\quad+V\int_L\frac{\partial\{xM_H(\infty)\}}{\partial x}dx\dot{X}_2(t) \quad ,
\end{aligned}
\tag{15}
$$

$$D_{2j} = V\int_L \left[x\frac{\partial\{xM_H(\infty)\}}{\partial x}\right] dx\dot{X}_1(t) - V\int_L \left[x\frac{\partial\{xM_H(\infty)\}}{\partial x}\right] dx\dot{X}_2(t) \quad , \tag{16}$$

$$\begin{aligned} E_{1j} = &-V\int_L\int_0^t \frac{\partial K_H(t-\tau)}{\partial x} X_1(\tau)d\tau dx \\ &+V\int_L\int_0^t \frac{\partial\{xK_H(t-\tau)\}}{\partial x} X_2(\tau)d\tau dx \\ &+2V\int_L\int_0^t K_H(t-\tau)X_2(\tau)d\tau dx \\ &+V^2\int_L \frac{\partial M_H(\infty)}{\partial x} dxX_2(t) \quad , \end{aligned} \tag{17}$$

$$\begin{aligned} E_{2j} = &-V\int_L\int_0^t \left[x\frac{\partial K_H(t-\tau)}{\partial x}\right] X_1(\tau)d\tau dx \\ &-V\int_L\int_0^t \left[x\frac{\partial\{xK_H(t-\tau)\}}{\partial x}\right] X_2(\tau)d\tau dx \\ &-2V\int_L\int_0^t xK_H(t-\tau)X_2(\tau)d\tau dx \\ &+V^2\int_L \frac{\partial\{xM_H(\infty)\}}{\partial x} dxX_2(t) \end{aligned} \tag{18}$$

F_{WV} shows the wave exiting force in heave (j=1) and moment in pitch (j=2). These are expressed as follows:

$$F_{WV1}(t) = F_{WV1C}\cos\sigma_E t - F_{WV1S}\sin\sigma_E t \quad , \tag{19}$$

$$\begin{aligned} F_{WV1C} = &2\rho g\zeta\int_L be^{-kT_m}\cos kxdx \\ &-\zeta\sigma_W\sigma_E\int_L e^{-kT_m}M_H(\sigma_E)\cos k\,x\,d \\ &-\zeta\sigma_W\int_L e^{-kT_m}N_H(\sigma_E)\sin kxdx \quad , \end{aligned} \tag{20}$$

$$\begin{aligned} F_{WV1S} = &2\rho g\zeta\int_L be^{-kT_m}\sin kxdx \\ &-\zeta\sigma_W\sigma_E\int_L e^{-kT_m}M_H(\sigma_E)\sin k\,x\,d \end{aligned}$$

$$+\zeta\sigma_W \int_L e^{-kT_m} N_H(\sigma_E)\cos k\,x\,d \quad , \tag{21}$$

$$F_{WV2}(t) = F_{WV2C}\cos\sigma_E t - F_{WV2S}\sin\sigma_E t \quad , \tag{22}$$

$$\begin{aligned} F_{WV2C} = & -2\rho g\zeta \int_L bxe^{-kT_m}\cos kxdx \\ & + \zeta\sigma_W\sigma_E \int_L e^{-kT_m} M_H(\sigma_E)x\cos kxdx \\ & + \zeta\sigma_W V \int_L e^{-kT_m} M_H(\sigma_E)\sin kxdx \\ & + \zeta\sigma_W \int_L e^{-kT_m} N_H(\sigma_E)x\sin kxdx \\ & - \zeta V\frac{\sigma_W}{\sigma_E}\int_L e^{-kT_m} N_H(\sigma_E)\cos kxdx \quad , \end{aligned} \tag{23}$$

$$\begin{aligned} F_{WV2S} = & -2\rho g\zeta \int_L bxe^{-kT_m}\sin kxdx \\ & + \zeta\sigma_W\sigma_E \int_L e^{-kT_m} M_H(\sigma_E)x\sin kxdx \\ & - \zeta\sigma_W V \int_L e^{-kT_m} M_H(\sigma_E)\cos kxdx \\ & - \zeta\sigma_W \int_L e^{-kT_m} N_H(\sigma_E)x\cos kxdx \\ & - \zeta V\frac{\sigma_W}{\sigma_E}\int_L e^{-kT_m} N_H(\sigma_E)\sin kxdx \quad , \end{aligned} \tag{24}$$

where, ζ is the wave amplitude, T_m is the averaged draft, and b is the half breadth of ship.

4.3 Comparison of Simulated Results with Observed Ship Motions

The CC method and the CI method reproduce observed ship motions using the coastal wave data. Here, the consideration of accuracy is focused on the pitch motion. Fig. 8 shows spectrums of simulated pitch motions with observed ones on July 30, 2004, off Cape Muroto. The relative wave direction is 135 degrees, which is in bow seas. It is determined from the observed main wave direction and the averaged ship course. Wave-exciting forces are calculated from Eqs. 19-24, using the observed waves observed by the Muroto GPS. It is necessary to define the significant amplitude and period of pitch, shown as $PA_{1/3}$ and PT_{mean}, respectively. In Fig. 8, the spectrum of pitch motion can be reproduced accurately by both methods. There is not a significant difference in all frequencies between the CC and CI methods. However, the CC method slightly overestimates the significant pitch amplitude. The CI method

underestimates the significant pitch period by 1.5s. Fig. 9 shows the spectrums of simulated and observed pitch motions on September 13, 2003, off the Kochi point. The relative wave direction is 75 degrees, which is between the quartering and beam seas. The ferry is off the Port of Kochi; thus, the coastal wave data observed on the Kochi point is used in this case. The figure shows that the CC method considerably underestimates the energy of the observed pitch motion. $PA_{1/3}$ of the CC method is 0.9 degrees, which is almost half of the observed 1.9 degrees. On the other hand, $PA_{1/3}$ of the CI method is 2.2 degrees, which is quite close to the observed motion. PT_{mean} is 9.7s, which is slightly smaller than the observed one of 10.8s. There is an obvious difference in the reproduced accuracy between the two methods here.

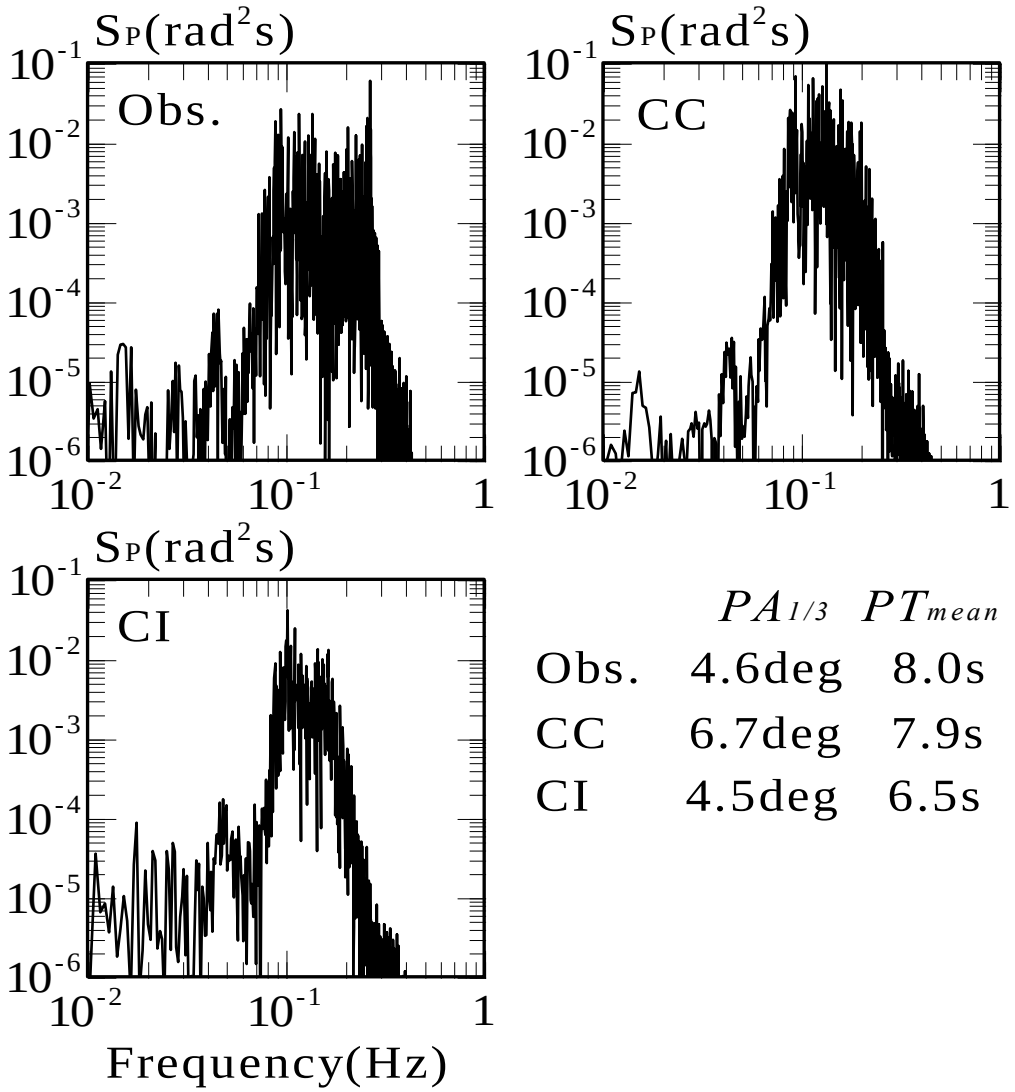

Fig. 8 Spectrums of simulated pitch motions with observed ones (July 30, 2004, Cape Muroto)

Numerical simulations are necessary to estimate ship motions using coastal waves. There are few studies on the verification of accuracy about observed ship motions

under severe sea conditions in time domain, despite of many studies on numerical analysis of ship motions (Kashiwagi, 1997 and 2000) in the field of naval architecture. Here, ship motions are reproduced for comparison with observed cases in time domain after two types of equations of motions are constructed.

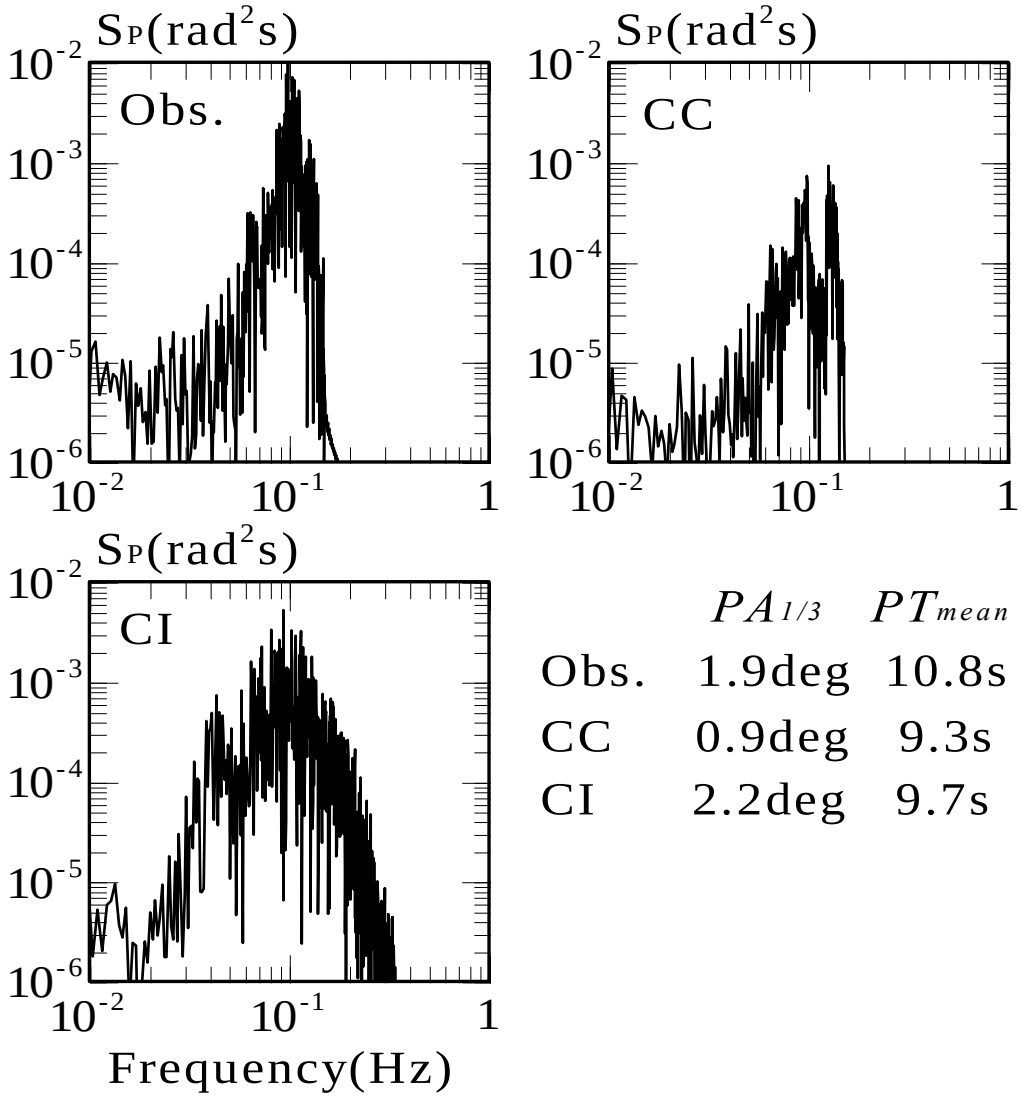

Fig. 9 Comparison of simulated pitch motions with observed ones (September 13, 2003, Kochi)

5. FACTORS CONTROLS REPRODUCTION ACCRACY OF SHIP MOTIONS UNDERWAY

It is shown that an obvious difference of reproduction appears in pitch motions in each simulation method, as shown in Fig. 9. Fig. 10 shows the computed result of the frequency response of the pitch motion in each wave direction and period. The ship speed is defined as 16 knots of averaged navigation speed on the basis of observed data.

The maximum amplitude appears at around 9s in head seas. Amplitudes range from 7 to 10s in other wave directions as well. The peak frequencies of pitch motion are consistent with those observed and shown in Fig. 6.

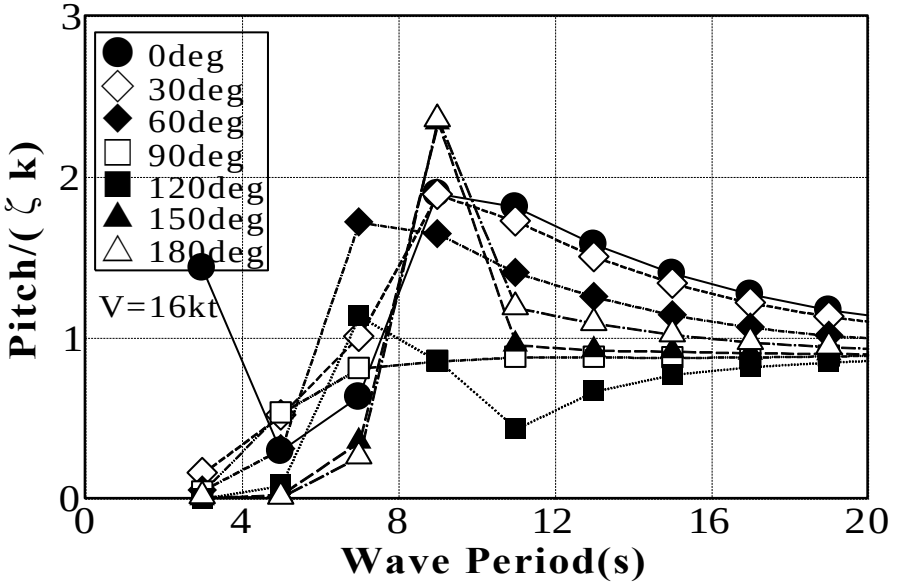

Fig. 10 Frequency response of pitch motion in each wave direction and wave period (Ship Velocity is 16 knots)

Shiraishi et al. (1999) have already shown that an evaluation of hydrodynamic forces is inadequate if these coefficients are represented at a significant wave period in equations of motions when we compute moored ship motions. Natural periods of surge, sway, or yaw motions are around 1-2 minutes long, as determined from the spring constant of mooring lines or fenders. There are multiple peaks of wave frequencies, especially in those during severe weather conditions. Moored ship motions are remarkable if the resonance appears in long periods of around 1-2 minutes. However, the CC method cannot reproduce this phenomenon because of the overestimation of the wave damping coefficient at the significant wave period. It is necessary to examine this point against the reproduction of ship motions underway. The values of the right-hand side term in Eqs. 2 and 12 are the same; therefore, the difference in pitch motions is attributed to the evaluation of hydrodynamic forces of the first and second terms on the left-hand side. Fig. 11 shows the computed wave damping coefficients in 0-20s. The natural period of pitch motion must be considered when assessing the reason for the different simulated results. It can be estimated as follows:

$$T_P = 2.007 \frac{\kappa_l}{\kappa_w} \sqrt{\frac{C_b d}{C_w}} \quad , \tag{25}$$

where T_P is the natural period of pitch motion, κ_l is the radius of gyration for the inertia moment in pitch motion, κ_W is the radius of gyration for the inertia moment on the water line, C_b is the block coefficient (=0.57), d is the draught (=4.5m), and C_W is the water line coefficient (=0.73). Here, the ratio of the radius of gyration, κ_l / κ_W, is defined as 1. The natural period of pitch, T_P, can be estimated as 3.8s. The figure shows that the wave damping coefficients decrease below 10s, especially around the natural period of pitch motion, 3.8s. The mean encounter period is transformed as follows:

$$T_{Emean} = \frac{1}{2\pi\sigma_{Emean}} \quad . \tag{26}$$

If the difference in pitch motions is attributed to the frequency of the property of hydrodynamic forces, the relationship between the natural period and the significant encounter period must be studied. Here, the difference of the time periods, *DTP*, is newly defined as follows:

$$DTP = \left| T_P - T_{Emean} \right| \quad . \tag{27}$$

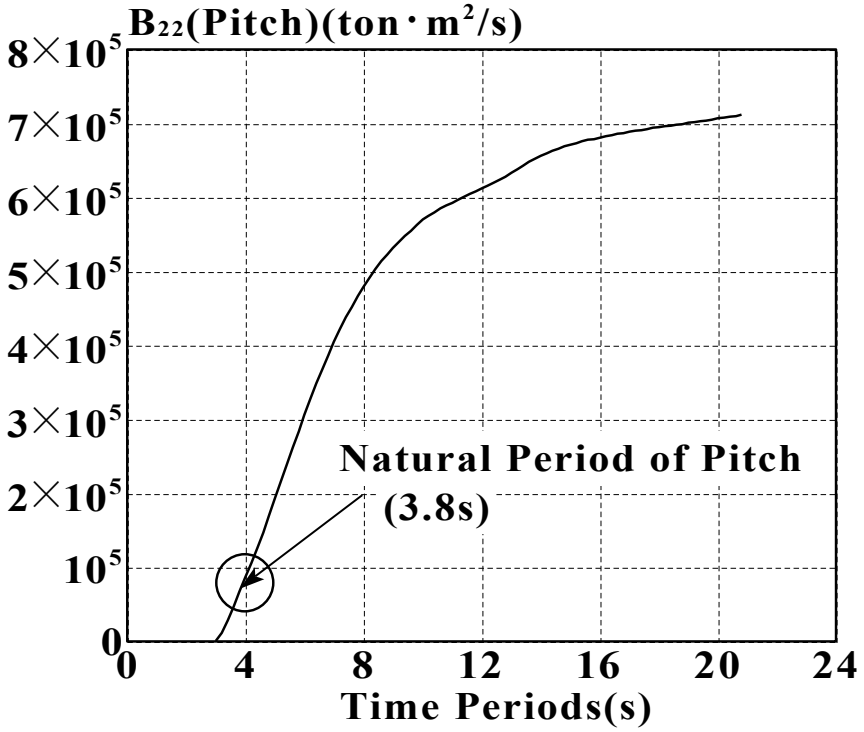

Fig. 11 Computed wave damping coefficients in the pitch mode

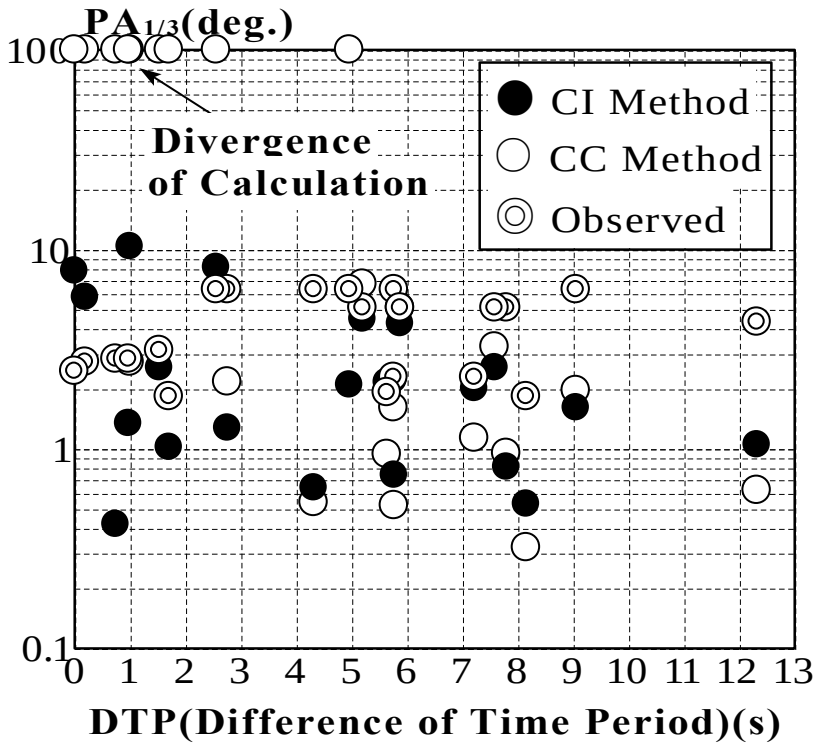

Fig. 12 Relationship between the time period and the ratio of the pitch amplitude

The relationship between the difference in the time period and the significant amplitudes in all cases is shown in Fig. 12. The pitch amplitudes are relatively similar in both simulation methods when the difference of time periods is larger than 2s. It indicates that the simulated results can reproduce observed ones to some extent. On the other hand, the pitch amplitudes become divergent in the CC method when the difference in the time periods is within 2s. This can be considered as the divergence phenomenon in resonance situations.

This result reveals that the CC method cannot reproduce the pitch motion in resonance frequencies. The pitch amplitudes are 0.4-10 degrees when the CI method is used in resonance frequencies. The simulated results are closer to the observed ones than those in the CC method. However, there are few cases in which the pitch amplitude completely agrees with observed one. It shows that the present accuracy is insufficient even when the CI method is used. In Fig. 11, the wave damping coefficients are very small around the natural period, which suggests that the damping moment of pitch motion is represented as almost zero in Eq. 2. If an external force around the natural period acts on a ship under these conditions, the diversion of pitch motion could be the result of the vibration resonance. The CI method considers the impulse response of wave damping coefficients in all frequencies. The second term in Eq. 12 is transformed into the function of time, not of frequency. That is the reason that the simulated results do not diverge in the CI method. As shown in Eq. 1, it is

necessary to consider the encounter frequency, such as the ship's velocity, the ship's course, or the wave direction to accurately reproduce the ship motions underway. The accuracy of wave data is very important, as well as the numerical simulation modeling. Using the coastal wave database of the NOWPHAS in this study, the practical effectiveness is more or less verified. Nevertheless, improving the accuracy of reproduction still presents some problems. First, the wave amplitudes are very different among nearby observation points, such as the Murotsu and the Muroto GPS. The topography will inevitably reduce the wave height beforehand. Second, the wave direction is often considered as only the main wave direction. As shown in Fig. 6, a complicated frequency property is observed as the combination of wind, waves and swells. They also have different patterns of wave directions or directional dispersions. More detailed information of wave direction is required to reproduce ship motions, although three wave directions are given in each frequency band in the present system. The data size becomes huge from the wave gauge if wave directions are considered as the multi-directional spectrum. Some problems still remain regarding data processing of coastal waves to improve the accuracy of ship motions underway.

6. CONCLUSIONS

(1) Ship motions underway for ferries become larger in open seas under atmospheric depressions as well as typhoons. Decisions regarding operations are made dependent on the potential damage to cargo. However, little information and mechanical systems are currently available to ship operators in stormy conditions.

(2) Pitch motions exceeding 5 degrees occur off Cape Muroto. Observational data indicates that the peak frequencies of pitch motion and observed coastal waves do not necessarily agree. In some cases, multiple peaks of waves are observed; therefore, the relationship of the frequencies is complex and does not lend itself to clear-cut decisions based on experience and intuition.

(3) Two methods of numerical simulations are established to compare the reproduction accuracy. The CC method underestimates the one of two observed pitch motions shown in Figs. 8-9, while the CI method can reproduce two observed cases.

(4) The significant amplitude of pitch is compared with the observed one, in the difference of time periods. The simulated results are not very different from each other when the difference in the time period exceeds 2s.

(5) The simulated results are quite different when the difference in the time period is less than 2s. The accuracy worsens in both methods. In particular, the simulated amplitudes diverge in the CC method in the resonance frequencies.

(6) In the CC method, hydrodynamic coefficients are represented at a specific frequency. The value of the wave damping coefficient rapidly decreases below 10s. The CC method simulates a pitch motion that is too large because the damping force is nearly zero at the time the pitch motion occurs. The value might be too large in Fig. 9,

however, the underestimation is explainable.

(7) The CI method considers the impulse response; therefore, the hydrodynamic forces do not depend on any frequency. This method yields more accurate results than the CC method. The results of this study show that the CI method is necessary to reproduce ship motions in resonance frequencies.

(8) The effectiveness of the coastal wave database, NOWPHAS, is shown for the prediction of pitch motion in significant values. However, coastal wave data are not encountered waves themselves, so the comparison of accuracy is in the frequency band. There are some studies that investigate data assimilation (Terada, et al., 2009). In the future, this method can be expected to estimate encounter waves from NOWPHAS data for the comparison with the time series.

(9) A new system that provides information about wave direction is needed; such a system should include a multi-directional spectrum. The study of wave direction is very complex, especially when wind and waves produce swells simultaneously.

(10) In future studies, a system for estimating impulse forces or collapse against cargo will need to be designed to determine when to cancel ferry services experiencing significant ship motions. Methods are needed to counteract or prevent impulsive force or the collapse of cargo due to pitch and roll motions.

ACKNOWLEDGEMENT

The authors are deeply indebted to the special support of Kochi Express Ferry, Ltd., regarding the field observations and interview research. Furthermore, we want to express appreciation to Dr. Go Kobayashi, Hiroshima National College of Maritime Technology, and Dr. Ik-Soon Cho, Korea Maritime University, for their support with the field observations. Furthermore, we express appreciation to Dr. Hiroyasu Kawai, the Port and Airport Research Institute, for providing information from the coastal wave database of NOWPHAS.

REFERENCES

Books:

Okusu, M. (1996). "Advances in Marine Hydrodynamics", *Computational Mechanics Publications*, 371p.

Ueda, S. (1984). "Analytical Method of Ship Motions Moored to Quay Walls and the Applications", *Technical Note of the Port and Harbour Research Institute, No.504,* 372p. (in Japanese)

Journals:

James, R.W. (1957). "Application of Wave Forecasts to Marine Navigation", *U.S. Naval Oceanographic Office*, SP-1.

Kashiwagi, M. (1997). "Numerical Seakeeping Calculations Based on Slender Ship

Theory," *Ship Technology Research (Schiffstechnik)*, Vol.4, No.4, pp.167-192.

Kobayashi, G., Mizui, S., Sasa, K., and Kubo, M. (2004). "Basic Research on the Safety Management of a Ferry Cargo in Rough Weather", *Proc. of the 14th International Conference of Offshore and Polar Engineering*, Vol.Ⅲ, pp.540-545.

Kobayashi, G., Kubo, M., Cho, I. and Hirayama, K. (2007). "Comparison Between Navigator's Wave Information and Calculation of Wave Deformation near Cape", *The Journal of Japan Institute of Navigation*, Vol.116, pp.121-127. (in Japanese)

Nagai, T., Sugahara, K., Hashimoto, N., Asai, T., Higashiyama, S., and Toda, K. (1994). "Introduction of Japanese NOWPHAS System and its Recent Topics", *Proc. of the International Conference on Hydro-Technical Engineering for Port and Harbor Construction*, pp.67-82.

Saito, K. and Higashi, H. (1992). "Time Domain Analysis of Ship Responses in Waves –Heave and Pitch Motions in Longitudinal Waves—", *Journal of the Society of Naval Architects of Japan*, Vol.172, pp.9-16. (in Japanese)

Sasa, K., Kubo, M., Shiraishi, S. and Nagai, T. (2003). "New Evaluation Method of Port Planning and Ship Operation From Viewpoint of Ship Motions Using New Observation System", *International Journal of Offshore and Polar Engineering*, Vol.13, No.2, pp.112-119.

Sasa, K., Kubo, M., Nagai, T., Yoneyama, H. and Shiraishi, S. (2005). "A Study on Difficulties of Entering and Departing Harbours due to Wave Induced Ship Motions", *International Journal of Offshore and Polar Engineering*, Vol.15, No.2, pp.117-124.

Sasa, K. and Nagai, T. (2006). "Basic Research on Stranding Accidents of Ships in Stormy Weathers From Viewpoint of Safety at Offshore Harbour Refuge", *Proc. of the 31st International Navigation Congress*, pp.1-12 (CD-ROM).

Shiraishi, S., Kubo, M., Ueda, S. and Sakakibara, S. (1996). "Countermeasure by Mooring System for Moored Ship Motions under Long Period Waves," *Proc. of the 5th Coastal Ocean Space Utilization*, pp 207-216.

Shiraishi, S., Sasa, K., Kubo M. and Sakakibara S. (1999). "A Study on Numerical Simulation Methods to Reproduce Long Period Ship Motions," *Proc of the 9th International Offshore and Polar Engineering Conference*, Vol 3, pp 536-543.

Terada, D., Kitagawa, G., Shiotani, S. and Kobayashi, E. (2009). "Estimation of a Maneuverability Index based on Data Assimilation", *Proc. of the Asia Navigation Conference 2009* , pp.165-170.

Article in Book Edited by Another Author:

Kashiwagi, M. (2000). "The State of the Art on Slender-Ship Theories of Seakeeping", *Proc. of 4th Osaka Colloquium on Seakeeping Performance of Ships (Osaka)*, pp.11-25.